Iterative Statistical Reconstruction Algorithm Based on C-C Data Model with the Direct Use of Projections Performed in Spiral Cone-beam CT Scanners

Robert Cierniak and Piotr Pluta

Institute of Computational Intelligence, Czestochowa University of Technology, Armii Krajowej 36, 42-200 Czestochowa, Poland,
{robert.cierniak, piotr.pluta}@iisi.pcz.pl

Abstract. This paper is concerned with the originally formulated 3D statistical model-based iterative reconstruction algorithm for spiral cone-beam x-ray tomography. The conception proposed here is based on a continuous-continuous data model, and a reconstruction problem is formulated as a shift invariant system. This algorithm significantly improves the quality of the subsequently reconstructed images, so allowing a decrease in the x-ray dose absorbed by a patient. The analytical roots of the algorithm proposed here permit a decrease in the complexity of the reconstruction problem in comparison with other model-based iterative approaches. In this paper, we proved that this statistical approach, originally formulated for parallel beam geometry, can be adapted for helical cone-beam geometry of scanner, with the direct use of projections. Computer simulations have shown that the reconstruction algorithm presented here outperforms conventional analytical methods with regard to the image quality obtained.

Keywords: Image reconstruction from projections, x-ray computed tomography, statistical reconstruction algorithm

1 Introduction

Nowadays, the most significant problem in medical computer tomography (CT) is the development of image reconstruction algorithms from projections which would enable the reduction of the impact of measurement noise on the quality of tomography images. It is argued that x-ray radiation is harmful to the health of patients being examined because it can lead to many serious illnesses [1], and this therefore creates a barrier to the development of this x-ray medical imaging technique. This kind of approach is intended to improve image quality and, in consequence, reduce the dose of X-ray radiation while at the same time preserving an appropriate level of quality in the tomography images. The concept has found its application in the form of statistical reconstruction algorithms. One of the most interesting from the scientific and practical point

of view, an approach, called MBIR (Model-Based Iterative Reconstruction), is presented in publications like [2], [3] and [4], where a probabilistic model of the measurement signals is described analytically (for more details see also [5] and [6]. The objective in those solutions was devised according to a discrete-discrete (D-D) data model (consequently, in 2010, this development had its debut under its commercial name Veo - CT Model-Based Iterative Reconstruction [7], [8]). This scheme has been selected in this case for one very obvious reason - the measurement noise can be modelled relatively easily, because each measurement is considered separately. Such a scheme adds significant calculative complexity to the problem. The time for image reconstruction becomes difficult from the practical point of view. For instance, if the image resolution is assumed to be I × I pixels, the complexity of the problem is of the level of $\mathrm{I} \times \mathrm{I} \times number\_of\_measurements \times number\_of\_cross-sections$ (in 3D tomography); a multiple of I to the power of four in total.

The difficulties mentioned above connected with the use of an methodology based on the D-D data model can be decreased by using a strategy of reconstructed image processing based on a continuous-continuous (C-C) data model. In previous papers we have shown how to formulate reconstruction problem consistent with the C-C mode and with the maximum-likelihood (ML) methodology for parallel scanner geometry [9], [10] and [11]. This strategy has been used for fan-beams [12], and finally for the spiral cone-beam scanner [13] and [14]. However, an approach to the reformulation of the reconstruction problem from parallel to real scanner geometries, called rebinning, was applied there. Much more popular 3D reconstruction methods, which are implemented in practice, are FDK (Feldkamp)-type algorithms that use projections obtained from spiral cone-beam scanners directly (see e.g. [15]). In this paper, we present a mathematical derivation of a method for the direct (i.e. without rebinning) adaptation of spiral cone-beam projections to the statistical analytical reconstruction algorithm originally formulated by us.

2 Adoption of the 2D Analytical Approximate Reconstruction Problem to the Helical Cone-beam Projections

Taking into consideration the definition of the two-dimensional inverse Fourier transform, and the frequential form of the relation between the original image of a cross-section of an examined object represented by function $\mu(x, y)$ and the image obtained after the back-projection operation $\tilde{\mu}(x, y)$, we obtain:

$$\tilde{\mu}(x, y) = \int_{-\infty}^{\infty} \int_{-\infty}^{\infty} \frac{1}{|f|} M(f_1, f_2)\, e^{j2\pi(f_1 x + f_2 y)} df_1 df_2, \tag{1}$$

which, after converting to polar coordinates and using the projection slice theorem (taking into account a full revolution of the projection system), takes the

form:

$$\tilde{\mu}(x,y) = \frac{1}{2}\int_{-\pi}^{\pi}\int_{-\infty}^{\infty} \bar{P}(f,\alpha^p)\, e^{j2\pi f(x\cos\alpha^p + y\sin\alpha^p)} df d\alpha^p. \tag{2}$$

Then, after transferring the projections into the spatial domain, and arranging the right hand side of the formula and changing the order of integration, we get the following formula:

$$\tilde{\mu}(x,y) = \frac{1}{2}\int_{-\infty}^{\infty}\int_{-\infty}^{\infty}\int_{-\pi}^{\pi} \bar{p}^p(s,\alpha^p)\, e^{j2\pi f(x\cos\alpha^p + y\sin\alpha^p - s)} d\alpha^p ds df, \tag{3}$$

where $\bar{p}^p(s,\alpha^p)$ are projections obtained in a hypothetical parallel scanner (after interpolation).

Next, after converting the attenuation function into polar coordinates, we obtain:

$$\tilde{\mu}(r\cos\phi, r\sin\phi) = \frac{1}{2}\int_{-\infty}^{\infty}\int_{-\infty}^{\infty}\int_{-\pi}^{\pi} \bar{p}^p(s,\alpha^p)\, e^{j2\pi f[r\cos(\alpha^p-\phi)-s]} d\alpha^p ds df. \tag{4}$$

In our considerations, we should also take into account the application of the interpolation function used during the back-projection operation, which should be placed appropriately (a frequency representation of this function) in the formula above, as follows:

$$\breve{\mu}(x,y) = \frac{1}{2}\int_{-\infty}^{\infty}\int_{-\infty}^{\infty}\int_{-\pi}^{\pi} INT(f)\, p^p(s,\alpha^p)\, e^{j2\pi f[r\cos(\alpha^p-\phi)-s]} d\alpha^p ds df. \tag{5}$$

After suitable transformation we obtain a relationship for the fan-beam image reconstruction method:

$$\breve{\mu}(x,y) = \frac{\mathrm{R}_f}{2}\int_{0}^{2\pi}\int_{-\beta_m}^{\beta_m} p^f\left(\beta,\alpha^f\right)\frac{\cos\beta}{\dot{u}^2}\int_{-\infty}^{\infty} INT(f)\, e^{j2\pi f\dot{u}\sin\left(\dot{\beta}-\beta\right)} df d\beta d\alpha^f, \tag{6}$$

where $p^f\left(\beta,\alpha^f\right)$ are projections obtained in a hypothetical fan-beam scanner, and

$$\dot{u} = \left(x\cos\alpha^f + y\sin\alpha^f\right)^2 + \left(R_f + x\sin\alpha^f - y\cos\alpha^f\right)^2. \tag{7}$$

There is a several serious drawbacks associated with the use of the fan-beam reconstruction method formulated like this. It stems from the dependence of equation (6) on the parameter $\dot{u}$, which poses certain practical problems when carrying out the calculations during the reconstruction process. Instead of a simple formula for the convolution kernel, it now becomes necessary to determine a different form of the kernel for every point of the object's cross-section. This is because $\dot{u}$ represents the distance of the point (r,ϕ) from the radiation source.

Therefore, by changing the angle α^f, we also change $\dot{u}$. The appropriate adjustment is based on a term in equation (6), which is reproduced here in a suitably amended form:

$$int\,(s) = \int_{-\infty}^{\infty} INT\,(f)\, e^{j2\pi f \dot{u} \sin\left(\dot{\beta}-\beta\right)} df. \tag{8}$$

In this equation, the integration is carried out with respect to the frequency f. The next step will be to make a substitution for f, using the following expression:

$$f^f = \frac{f \cdot \dot{u} \cdot \sin\beta}{\mathrm{R}_f \cdot \beta}. \tag{9}$$

If at the same time we change the limits of integration, the convolving function will be modified to:

$$int^f\,(\beta) = \frac{\mathrm{R}_f \cdot \beta}{\dot{u} \cdot \sin\beta} \int_{-\infty}^{\infty} INT\left(\frac{f^f \cdot f_0}{f_0^f}\right) e^{j2\pi f^f \mathrm{R}_f \beta} df^f, \tag{10}$$

where

$$f_0^f = \frac{f_0 \cdot \dot{u} \cdot \sin\beta}{\mathrm{R}_f \cdot \beta}. \tag{11}$$

Unfortunately, even here we encounter problems caused by the dependence of the cut-off frequency f_0^f on the parameter $\dot{u}$. On the other hand, if we were to establish a constant value for f_0^f it would mean that the reconstruction process for the point (r, ϕ) would have a different resolution (determined by the value of the cut-off frequency f_0) for every angle α^f. However, if we put aside the assumption of uniform resolution for the resulting reconstructed image, then, by manipulating the values $\dot{u}$ and f_0, the varying value of f_0^f can be fixed as:

$$f_0^f = \mathrm{f}_0^f = \frac{1}{\mathrm{R}_f \cdot \Delta_\beta}. \tag{12}$$

Let us assume that we apply a linear interpolation function in formula (6). The frequency form of the linear interpolation function is given by this formula:

$$INT_L\,(f) = \frac{\sin^2\left(\pi f \Delta_s\right)}{\left(\pi f \Delta_s\right)^2}. \tag{13}$$

Taking into account in the formula (10) the proposed interpolation function given by (13), we obtain the following relation:

$$int_L^f\,(\beta) = \frac{\mathrm{R}_f \cdot \beta}{\dot{u} \cdot \sin\beta} \begin{cases} \frac{1}{\Delta_s'}\left(1 - \frac{\mathrm{R}_f|\beta|}{\Delta_s'}\right) & \text{for } |\beta| \le \Delta_s' \\ 0 & \text{for } |\beta| \ge \Delta_s' \end{cases}, \tag{14}$$

where $\Delta_s' = f_0 / f_0^f$, and next, bearing in mind relations (12), it leads immediately to:

$$int_L^f\,(\beta) = \frac{\beta}{\dot{u} \cdot \sin\beta} \begin{cases} \frac{\Delta_s}{\Delta_\beta}\left(1 - \frac{\Delta_s|\beta|}{\Delta_\beta}\right) & \text{for } |\beta| \le \frac{\Delta_\beta}{\Delta_s} \\ 0 & \text{for } |\beta| \ge \frac{\Delta_\beta}{\Delta_s} \end{cases}. \tag{15}$$

Finally, if we assume that $\Delta_s = 1$, it gives

$$int_L^f(\beta) = \frac{\beta}{\dot{u} \cdot \sin\beta} int_L(\beta), \tag{16}$$

where

$$int_L(\beta) = \begin{cases} \frac{1}{\Delta_\beta}\left(1 - \frac{|\beta|}{\Delta_\beta}\right) & \text{for } |\beta| \leq \Delta_\beta \\ 0 & \text{for } |\beta| \geq \Delta_\beta \end{cases}. \tag{17}$$

In consequence, returning to the formula (8), we obtain

$$\breve{\mu}(x,y) = \frac{1}{2}\int_0^{2\pi}\int_{-\beta_m}^{\beta_m} p^f\left(\beta, \alpha^f\right) \frac{\mathrm{R}_f \cos\beta}{2\dot{u}} \frac{\Delta\beta}{\sin\Delta\beta} int_L(\Delta\beta)\, d\beta d\alpha^f. \tag{18}$$

Fortunately, we can linearize relation (18) by considering expressions inside the integration, namely $\frac{\Delta\beta}{\sin\Delta\beta}$.

In the case of linear interpolation we use only line of integrals from the neighborhood of a given pixel (x, y), then $\Delta\beta \leq \Delta_\beta$, and $\sin\Delta\beta \approxeq \Delta\beta$. Additionally, it is possible to omit the term $\frac{\mathrm{R}_f \cos\beta}{2\dot{u}}$ taking into account the fact that each projection value $p^f\left(\beta, \alpha^f\right)$ has its equivalent $p^f\left(-\beta, \alpha^f + \pi + 2\beta\right)$. Because of this we can notice that the sum of this pair of projections is proportional to $\frac{\dot{u}_1+\dot{u}_2}{4\dot{u}_1} + \frac{\dot{u}_1+\dot{u}_2}{4\dot{u}_2} = \frac{(\dot{u}_1+\dot{u}_2)^2}{4\dot{u}_1\dot{u}_2}$. This means that for $\dot{u}_1 \approxeq \dot{u}_2$ this factor is equal to 1, and finally, we can write

$$\breve{\mu}(x,y) \approxeq \frac{1}{2}\int_0^{2\pi}\int_{-\beta_m}^{\beta_m} p^f\left(\beta, \alpha^f\right) int_L(\Delta\beta)\, d\beta d\alpha^f, \tag{19}$$

which is consistent with a form of the formula of the back-projection operation for parallel beams.

Moreover, if we assume that rays, i.e. integral lines defining $p^f\left(\beta, \alpha^f\right)$, from the hypothetical fan-beam geometry pass through almost the same tissues as rays from cone-beam geometry ($p^h\left(\beta, \alpha^h, z_k\right)$), the projection values associated with these rays will be related to the corresponding path lengths through the tissues. Because of this, we can derive the correction factor by using the following relation:

$$p^f\left(\beta, \alpha^f\right) = p^h\left(\beta, \alpha^h, z_k\right) CORR = p^h\left(\beta, \alpha^h, z_k\right) \frac{R_{fd}}{\sqrt{R_{fd}^2 + z_k^2}}, \tag{20}$$

where R_{fd} is the source-to-detector distance; z_k is the transverse position on the screen where a given ray is detected.

The geometry of this method of determining the correction factor is shown in Figure 1.

Finally, formula (20) can be used directly to obtain a reference image for the analytical statistical iterative reconstruction algorithm presented by the formula (1), which was originally formulated for parallel beam scanner geometry, as follows

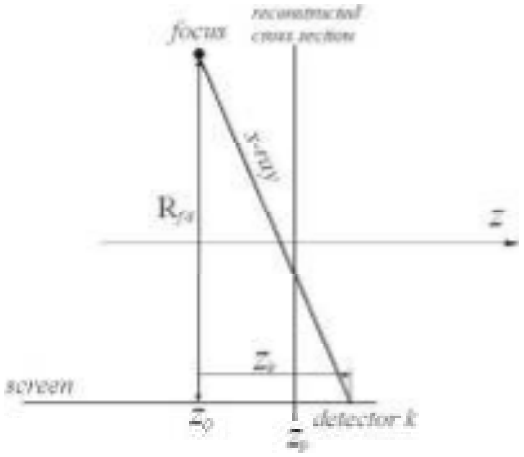

Fig. 1. The geometry of the cosine correction factor

$$\breve{\mu}\left(x,y\right) \approxeq \frac{1}{2}\int\limits_{0}^{2\pi}\int\limits_{-\beta_m}^{\beta_m} CORR \cdot p^{h}\left(\beta,\alpha^{h},z_k\right) int_L\left(\Delta\beta\right) d\beta d\alpha^{f}. \tag{21}$$

There exists in statistics a method known in the literature as a ML estimation, which find its implementation also to solve a reconstruction problems methods (see e.g. [16]). The objective in those solutions was devised according to a discrete-discrete (D-D) data model. As was mentioned, this scheme has some very serious drawbacks, and has been selected for one very obvious reason - the measurement noise can be modelled relatively easily, because each measurement is considered separately. We propose here the optimization formula which is consistent with C-C data model, in the following form:

$$\mu_{\min} = \arg\min_{\mu}\left(\int\limits_{x\in X}\int\limits_{y\in Y}\left(\int\limits_{\bar{x}\in X}\int\limits_{\bar{y}\in Y}\mu\left(\bar{x},\bar{y}\right)\cdot h_{\Delta x,\Delta y}d\bar{x}d\bar{y} - \breve{\mu}\left(x,y\right)\right)^{2} dxdy\right), \tag{22}$$

where coefficients $h_{\Delta i,\Delta j}$ can be precalculated according to the following relation:

$$h_{\Delta i,\Delta j} = \frac{1}{2}\int\limits_{0}^{2\pi} int\left(\Delta i\cos\psi\Delta_\alpha + \Delta j\sin\psi\Delta_\alpha\right) d\beta, \tag{23}$$

and $\tilde{\mu}\left(x,y\right)$ is an image obtained by way of a back-projection operation; $int\left(\Delta s\right)$ is an interpolation function used in the back-projection operation.

The above presented shift-invariant system is much better conditioned than qua-dratic form used in other approaches [17], and can be a starting point for

the design of a 3D iterative reconstruction algorithm for spiral cone-beam scanner geometry. In our case, this algorithm is based on the one of the principal reconstruction methods devised for the cone-beam spiral scanner, i.e. the generalized FDK algorithm [18]. Generally, proposed by us statistical reconstruction algorithm consists of two steps, namely: an interpolation described by relation (21) and an iterative reconstruction procedure according to formula (22).

3 Experimental Results

In our computer simulations, we have used projections obtained from a helical scanner Somatom Definition AS+ (Siemens Healthcare), with the following parameters: reference tube potentia 120kVp and quality reference effective 200mAs, $R_{fd} = 1085.6mm$ (SDD - Source-to-Detector Distance); $R_f = 595$mm (SOD - Source-to-AOR Distance); number of views per rotation $\Psi = 1152$; number of pixels in detector panel 736; detector dimensions 1.09mm $\times$ 1.28mm. During the experiments, the size of the processed image was fixed at 512×512 pixels. The matrix of the coefficients $h_{\Delta i,\Delta j}$ were precomputed before the reconstruction process was started, and these coefficients were fixed for the subsequent processing. The image obtained after back-projection operation was then subjected to a process of reconstruction (optimization) using an iterative procedure. The starting point of this procedure was chosen as a result of using a reconstruction FBP algorithm. It is worth noting that our reconstruction procedure was performed without any regularization regarding the objective function described by (22). The iterative reconstruction procedure was implemented for a computer with 10 cores, i.e. with an Intel i9-7900X BOX/3800MHz processor (the iterative reconstruction procedure was implemented at assembler level), and using a GPU type nVidia Titan V. According to an assessment of the quality of the obtained images by a radiologist, 8000 iterations are enough to provide an acceptable image. The same results were achieved for both hardware implementations after 7.44s and 7.73s, for the CPU and GPU implementations, respectively. It is worth emphasizing that reconstruction process cab be performed for every cross-section image separately, and a specific image requested by a doctor is ready for diagnostics after the above mentioned time. In the case of the referential approach this time is from 10 up to 90 minutes depending on the number of the simultaneously reconstructed cross-sections [8], [19].

All of the measurement data was obtained thanks to the organizers of the Low Dose CT Grand Challenge [20]. The results obtained by the participants in this competition were evaluated based on the correctness of diagnoses made with a reduced dose of radiation. In our experiments, we reduced the radiation using half the number of views (sparse sampling with limited projections of views). We used a hundred images, with and without pathological changes. The reconstructed images were then assessed by a radiologist: he marked lesions in these images according to his subjective opinion. Table 1 shows tabulated scores, where the above-mentioned diagnoses are related to the presence of true lesions (as given by the organizers of the Low Dose CT Grand Challenge), i.e. the table

shows the numbers of true positive cases (at least one lesion correctly marked in a case with lesions), true negative cases (no lesions marked in a case with no lesions), false positive cases (at least one lesion marked in a case with no lesions) and false negative cases (no lesions marked in a case that had lesions).

Table 1. Results of the diagnoses made by a radiologist with a dose of radiation reduced by half

Category	true negative	true positive	false negative	false positive
	62	21	8	9

Sample views of the reconstructed images are presented in Figures 2 and 4 (where a reduction of x-ray dose absorbed by a patient is simulated: half the standard dose). For comparison, the images reconstructed by a traditional Feldkamp reconstruction algorithm are also presented, for the same, half standard dose (Figures 3 and 5).

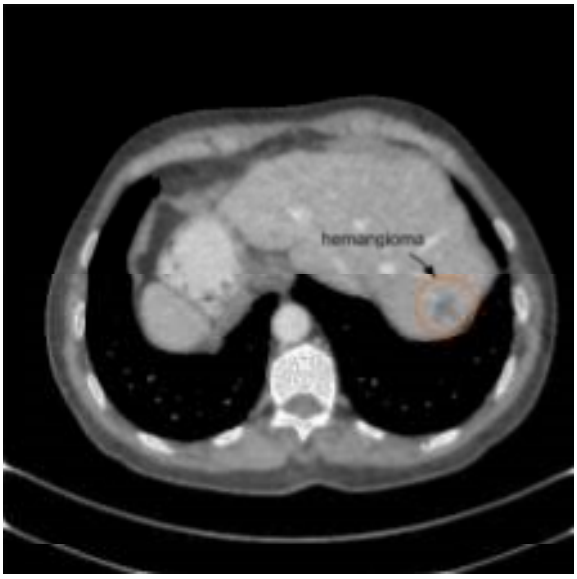

Fig. 2. View of the reconstructed image using the statistical method presented in this paper: a case with a large pathological change in the liver (hemangioma)

Fig. 3. View of the reconstructed image using the standard FBP: a case with a large pathological change in the liver (hemangioma)

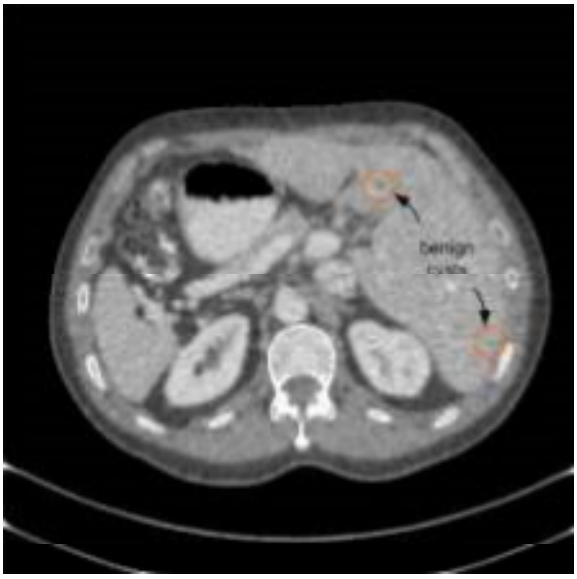

Fig. 4. View of the reconstructed image using the statistical method presented in this paper: a case with small pathological changes in the liver (bening cysts)

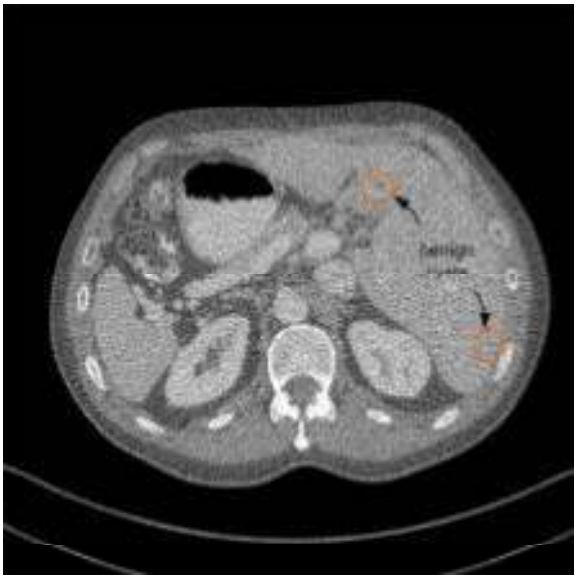

Fig. 5. View of the reconstructed image using the standard FBP: a case with small pathological changes in a the liver (bening cysts)

4 Conclusion

We have shown in this paper fully feasible statistical reconstruction algorithm for helical cone-beam scanner. It is proved that this statistical approach, originally formulated for parallel beam geometry, can be adapted for helical cone-beam geometry, without any filtration and any rebinning. Simulations have been conducted, which prove that our reconstruction method can be very fast (first of all thanks to the use of FFT algorithms) and gives satisfactory results with suppressed noise, without introducing any additional regularization term, using only an early stopping regularization strategy.

Acknowledgement. The authors thank Dr. Cynthia McCoullough and the American Association of Physicists in Medicine for providing the Low-Dose CT Grand Challenge dataset.

This work was partly supported by The National Centre for Research and Development in Poland (Research Project POIR.01.01.01-00-0463/17).

References

1. Mathews, J.D., et al.: Cancer risk in 680 people expose to computed tomography scans in childhood or adolescent: data inkage study of 11 million Australians. British Medical Journal 2013, 346:f2360.
2. Bouman, C., Sauer, K.: A unified approach to statistical tomography using coordinate descent optimization. IEEE Tran. Image Processing 5, 480–492 (1996)
3. Thibault, J.-B., Sauer, K.D., Bouman, C.A., Hsieh, J.: A three-dimensional statistical approach to improved image quality for multislice helical CT. Med. Phys. 34, 4526–4544 (2007)
4. Zhou, Y., Thibault, J.-B, Bouman, C.A., Hsieh, J., Sauer, K.D.: Fast model-based x-ray CT reconstruction using spatially non-homogeneous ICD optimization. IEEE Tran. Im. Proc. 20, 161–175 (2011)
5. Ding, Q., Long, Y., Zhang, X., Fessler, J.A.: Modeling mixed Poisson-Gaussian noise in statistical image reconstruction for x-ray CT. Proc. of the 4th International Conference on Image Formation in X-Ray Computed Tomography, July 18-22, Bamberg, Germany, 399–402 (2016)
6. Hoffman, J.M., Hsieh, S.S., Noo, F., McNitt-Gray, M.F.: FreeCT_ICD: Free, open-source MBIR reconstruction software for diagnostic CT, Proc. of the 5th International Conference on Image Formation in X-Ray Computed Tomography, May 20-23, Salt Lake City, USA, 252–254 (2018)
7. Thibault, J.-B.: Veo: CT model-based iterative reconstruction. http://www.gehealthcare.com (2010)
8. Geyer, L.L., et al.: State of the art: iterative CT reconstruction techniques. Radiology 276, 339–357 (2015)
9. Cierniak, R.: A new approach to tomographic image reconstruction using a Hopfield-type neural network. Int. J. Artificial Intelligence in Med. 43, 113–125 (2008)
10. Cierniak, R.: A new approach to image reconstruction from projections problem using a recurrent neural network. Int. J. Applied Math. Comp. Sc. 183, 147–157 (2008)
11. Cierniak, R.: New neural network algorithm for image reconstruction from fan-beam projections. Neurocomputing 72, 3238–3244 (2009)
12. Cierniak, R.: An analytical iterative statistical algorithm for image reconstruction from projections. Applied Mathematics and Computer Science 24, 7–17 (2014)
13. Cierniak, R.: A three-dimensional neural network based approach to the image reconstruction from projections problem. In: Rutkowski, L., Tadeusiewicz, R., Zadeh, L.A., Żurada, J. (eds.) LNCS 6113, 505–514. Springer, Heidelberg (2010)
14. Cierniak, R., Knas, M.: Ultrafast Iterative Model-based Statistical 3D Reconstruction Algorithm for X-ray Computed Tomography. 4th Int. Conf. Information Technologies in Biomedicine, Kamien Sląski, 2-4.VI.2014, Advances in Inteligent Systems and Computing 283, 187–196 (2014)

15. Cierniak, R., Knas, M.: Ultrafast Fully Analytical Iterative Model-based Statistical 3D Reconstruction Algorithm. In Proc. of the 12th Int. Meeting on Fully Three-Dimensional Image Reconstruction in Radiology and Nuclear Medicine, Lake Tahoe, 16-21.VI.2013, pp. 521-524 (2013)
16. Sauer, K., Bouman, C.: A local update strategy for iterative reconstruction from projections. IEEE Tran. Signal Processing 41, 534–548 (1993)
17. Cierniak, R., Lorent, A.: Comparison of algebraic and analytical approaches to the formulation of the statistical model-based reconstruction problem for x-ray computed tomography. Computerized Medical Imaging and Graphics 52, 19–27 (2016)
18. Feldkamp, L.A., Davis, L.C., Kress, J.W.: Practical cone-beam algorithm. J. Opti. Soc. America 1(A) 9, 612–619 (1984)
19. Nelson, R.C., Feuerlein, S., Boll, D.T.: New iterative reconstruction techniques for cardiovascular computed tomography: how do they work, and what are the advantages and disadvantages? Med. Phys. 5, 286–292 (2011)
20. www.aapm.org/GrandChallenge/LowDoseCT